JACS Au
AN OPEN ACCESS JOURNAL OF THE AMERICAN CHEMICAL SOCIETY

pubs.acs.org/jacsau
Article

Integrating Au Catalysis and Engineered Amine Dehydrogenase for the Chemoenzymatic Synthesis of Chiral Aliphatic Amines

Published as part of JACS Au virtual special issue "Biocatalysis in Asia and Pacific".

Jianqiao Liu, Jing Bai,* Yunting Liu, Liya Zhou, Ying He, Li Ma, Guanhua Liu, Jing Gao, and Yanjun Jiang*

Cite This: JACS Au 2024, 4, 2281−2290
Read Online

ACCESS | Metrics & More | Article Recommendations | Supporting Information

ABSTRACT: Direct synthesis of aliphatic amines from alkynes is highly desirable due to its atom economy and high stereoselectivity but still challenging, especially for the long-chain members. Here, a combination of Au-catalyzed alkyne hydration and amine dehydrogenase-catalyzed (AmDH) reductive amination was constructed, enabling sequential conversion of alkynes into chiral amines in aqueous solutions, particularly for the synthesis of long-chain aliphatic amines on a large scale. The production of chiral aliphatic amines with more than 6 carbons reached 36−60 g/L. A suitable biocatalyst [*Pt*AmDH (A113G/T134G/V294A)], obtained by data mining and active site engineering, enabled the transformation of previously inactive long-chain ketones at high concentrations. Computational analysis revealed that the broader substrate scope and tolerance with the high substrate concentrations resulted from the additive effects of mutations introduced to the three gatekeeper residues 113, 134, and 294.

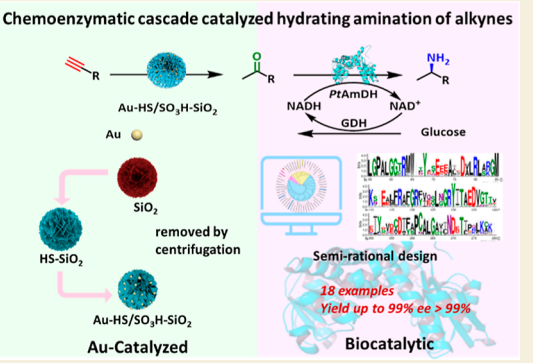

KEYWORDS: *chiral aliphatic amines, chemoenzymatic, alkyne hydration, amine dehydrogenase, reshaping pocket*

1. INTRODUCTION

Chiral aliphatic amines are key intermediates in the synthesis of various antistatic agents, pigment dispersants, metal preservatives, and drugs.[1−7] In 2019, nearly half of the small molecule drugs among the top 200 best-selling drugs contained a chiral aliphatic amine as key building blocks.[8] (Figure 1) The market for aliphatic amines is anticipated to be the most rapidly expanding sector within the amine market, with an estimated valuation of $2.9 billion by the year 2025.[9] Nonetheless, in contrast to the well-established methodologies for aromatic amines, the synthesis of chiral aliphatic amines remains notably arduous, particularly for those with elongated carbon chains. Therefore, the development of a straightforward and efficient synthetic approach is of significant interest.

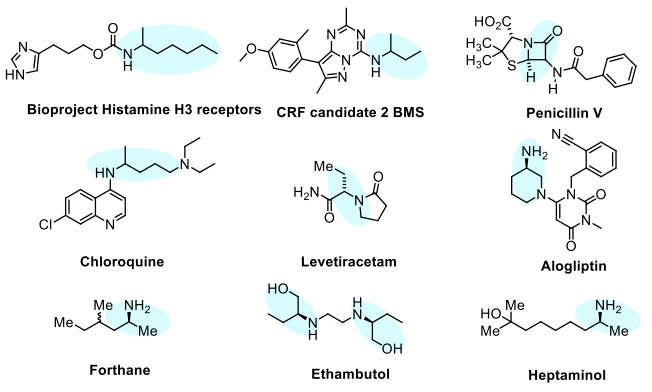

Figure 1. Pharmaceuticals and biologically active molecules containing aliphatic amine building blocks.

Several chemical methods have been developed to synthesize aliphatic amines. Maulide et al.[10] developed a hydrated amination reaction of ynamides/thioalkynes to synthesize α-amino acid derivatives using sulfamides as nitrogen sources. (Figure 2A) Fu et al.[8] designed a streamlined method to produce the chiral amines and their derivatives via nickel-catalyzed conversion of enamides and enecarbamates. Kempe et al.[11] reported the conversion of aliphatic compounds to primary amines catalyzed by an iron-based catalyst. However, these synthetic reactions remain limited due to poor selectivity and harsh reaction conditions.[12] To address this challenge, the biocatalytic synthesis of chiral amines offers

Received: March 11, 2024
Revised: May 25, 2024
Accepted: May 28, 2024
Published: June 10, 2024

https://doi.org/10.1021/jacsau.4c00222
JACS Au 2024, 4, 2281−2290

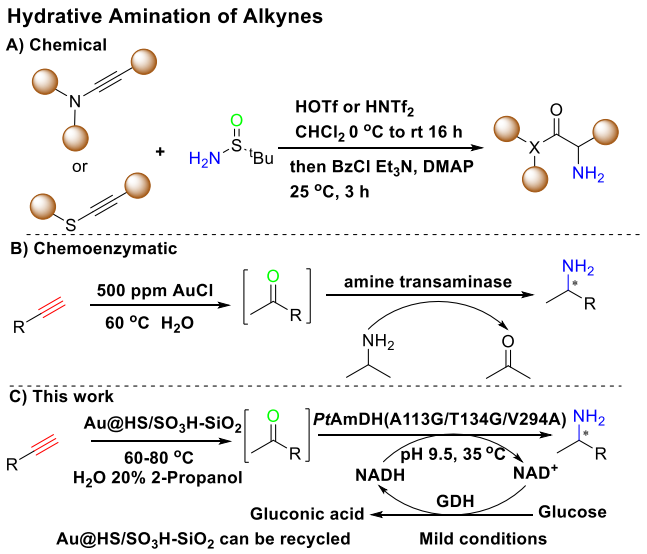

Figure 2. Methods for hydrating and aminating alkynes.

sustainable and environmentally friendly pathways, with a focus on reactions catalyzed by amine dehydrogenases (AmDHs), which exhibit several features indicative of an ideal process, including the direct utilization of cheap ammonia as amino donors and the production of water as the sole byproduct.[13] AmDHs are primarily acquired through two distinct pathways: (1) via the discovery of novel natural AmDHs, and (2) through the engineering of amino acid dehydrogenases (AADHs).[13] Despite the fact that many AmDHs have been studied, there are few reports on the asymmetric synthesis of long-chain aliphatic amines. A mutant *Lf*AmDH-M3 (K68S/A113G/T134G/N261L) from *Lysinibacillus fusiformis* constructed by Chen et al.[14] showed catalytic activity on several long-chain aliphatic ketones. Franklin et al.[15] developed a variant L-AmDH-TV$_{L39A/A112G/T133G}$ by introducing three additional mutations to the previously reported AmDH from *Geobacillus stearothermophilus* (*Gs*L-AmDH), which can catalyze the transformation of 2-decanone and 5-methyl-2-octanone to the corresponding chiral amines. Nevertheless, these synthetic reactions were mainly performed at low substrate concentrations. Thus, the mining of a new AmDH for long-chain aliphatic substrates with a higher tolerance to high substrate concentrations is still urgent.

Beyond the efficient biocatalysts, for the large-scale synthesis of chiral amines, the development of new synthetic methods using low-cost raw materials presents more practical advantages in industrial production. Alkynes are easily available and commonly used as building blocks in organic synthesis,

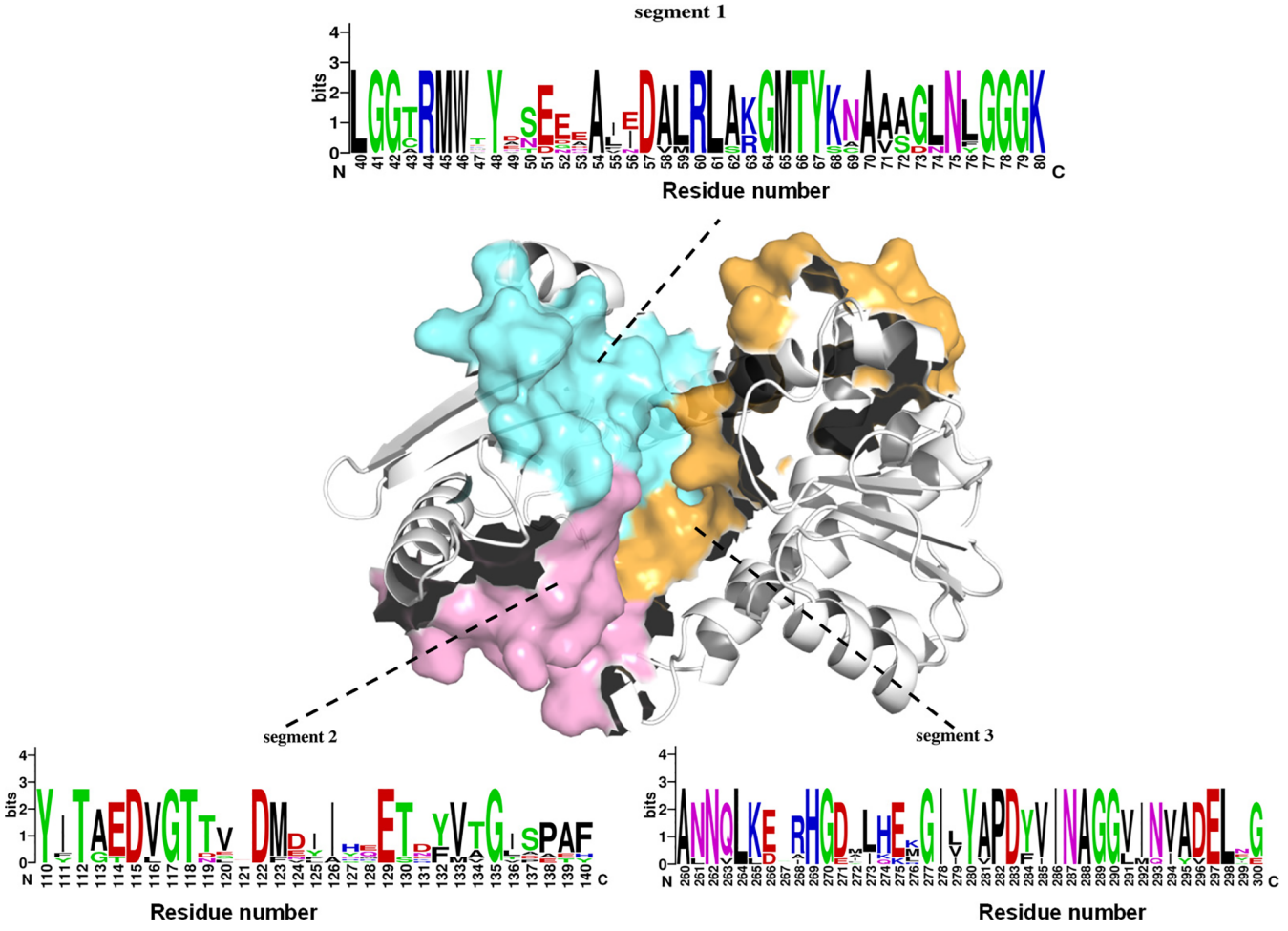

Figure 3. Structural comparison of amino acid dehydrogenases (AADHs). Analysis of the active sites of AADHs; the active site was divided into three segments. Sequence logos were generated from a multiple sequence alignment of 8 natural AADHs previously using Weblogo3 (https://weblogo.berkeley.edu/logo.cgi).

https://doi.org/10.1021/jacsau.4c00222
JACS Au 2024, 4, 2281−2290

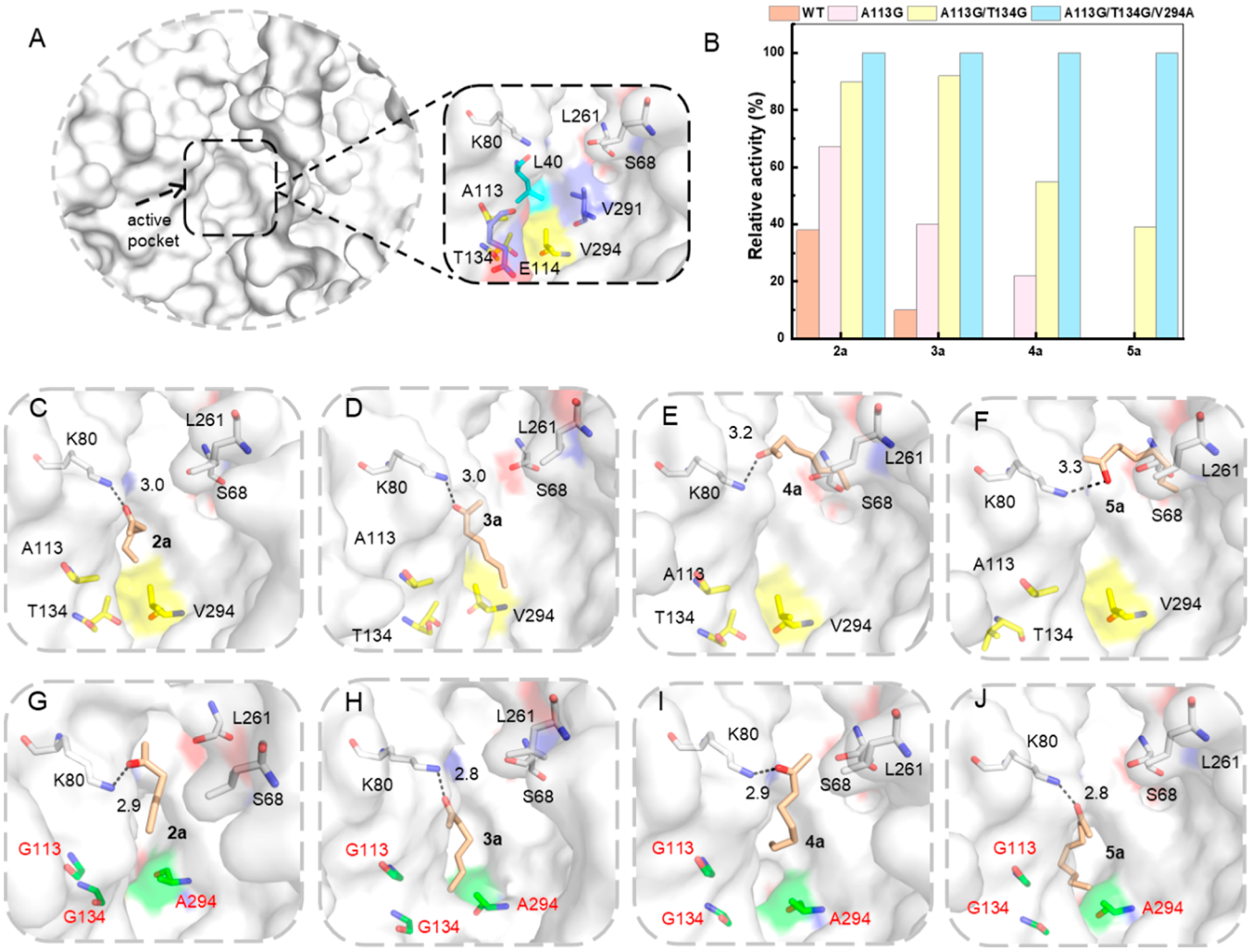

Figure 4. (A) Model of the active pocket. (B) Relative activity of *Pt*AmDH and engineered mutants toward substrates **2a**−**5a**. (C) Illustration of the substrate-binding cavities of *Pt*AmDH and its mutant. *Pt*AmDH-M0 with docked substrate **2a**. (D) *Pt*AmDH-M0 with docked substrate **3a**. (E) *Pt*AmDH-M0 with docked substrate **4a**. (F) *Pt*AmDH-M0 with docked substrate **5a**. (G) *Pt*AmDH (A113G/T134G/V294A) with docked substrate **2a**. (H) *Pt*AmDH (A113G/T134G/V294A) with docked substrate **3a**. (I) *Pt*AmDH (A113G/T134G/V294A) with docked substrate **4a**. (J) *Pt*AmDH (A113G/T134G/V294A) with docked substrate **5a**. Residues surrounding the substrate-binding pocket are shown in surface representation, and the substrates are shown as wheat and red sticks. Residues 113, 134, and 294 are highlighted in red.

which can be converted to ketones via metal-catalyzed alkyne hydration reactions.[16,17] Given the toxicity of the initial catalysts Hg(II) salts, many other metals were developed for the hydration of alkynes, such as Ag(I), Pt(II) and Au(III), but were found to be less efficient.[18−21] Until the introduction of Au(I) as catalysts by Teles et al.,[22] the research on the Au-catalyzed alkyne hydration reactions has attracted more attention. Nolan et al.[23] designed a (IPr)$AuBr_3$/MeOH system, which showed good catalytic performance for electron-rich aromatic terminal alkynes but low activity for aliphatic alkynes. Zuccaccia et al.[24] used cationic NHC gold as catalysts to achieve the hydration of alkynes under solvent-, silver-, and acid-free conditions, and the yield of ketones was up to 99%. Dutta and Phukan[25] developed the $CoFe_2O_4$−SiO_2−SH−Au(0) nanocatalyst, which showed excellent catalytic activity for the hydration of alkyl and aryl alkynes and can be reused many times through magnetic recovery. Thus, the development of Au-catalyzed hydration reactions for converting aliphatic alkynes to various aliphatic ketones is feasible.

Furthermore, the cascade reaction coupling the alkyne hydration reactions and enzymatic reductive amination reactions in one pot is worth considering from an industrial application standpoint. This approach not only utilizes inexpensive raw materials but also streamlines operational procedures. One significant challenge within this process lies in determining the compatibility between metal-catalyzed reactions and biocatalytic processes.[26] Mathew et al.[27] converted alkynes to ketones using AuCl as catalysts in the organic reaction mixture [DMSO/H_2O (98:2)], and the products were further converted to the corresponding amines by a transaminase. (Figure 2B) Recently, Gotor-Fernández and coworkers designed a sequential one-pot strategy utilizing Au(I) catalysis and amine transaminase for the synthesis of chiral amines.[28] These reports mainly focused on the synthesis of aromatic amines, as well as required organic solvents as reaction media and expensive Au/carbene complexes as catalysts. Given the increasing demand for long-chain aliphatic amines, the design of new cascade systems to synthesize the chiral aliphatic amines in aqueous solutions continues to be highly desirable.

https://doi.org/10.1021/jacsau.4c00222
JACS Au 2024, 4, 2281−2290

Table 1. Specific Activity of *Pt*AmDH-M0 and Its Mutants toward Aliphatic Ketones with Varied Chain Lengths

Entry	Mutant	Specific activity ($U/g_{protein}$) [a]				
		 (1a)	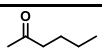 (2a)	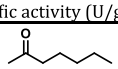 (3a)	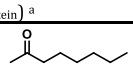 (4a)	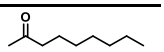 (5a)
1	*Pt*AmDH-M0	532.5	298.2	78.1	n.d.[b]	n.d.
2	L40A	257.2	115.1	29.4	n.d.	n.d.
3	L40G	n.d.	n.d.	n.d.	n.d.	n.d.
4	A113G	387.2	478.4	320.4	42.5	n.d.
5	T134G	402.5	367.2	137.1	22.9	n.d.
6	V291A	529.5	342.4	97.4	n.d.	n.d.
7	V291G	522.2	325.4	80.2	n.d.	n.d.
8	V294G	504.5	330.1	88.2	n.d.	n.d.
9	V294A	514.2	354.8	92.1	15.4	n.d.
10	A113G/T134G	224.1	705.9	725.7	105.2	89.2
11	A113G/T134G/V294A	227.2	786.7	791.4	192.1	152.8

[a]Specific activity was measured in $NH_4Cl/NH_3{\cdot}H_2O$ buffer (2 M, pH 9.5) containing 0.2 mM NADH and 20 mM substrate at 35 °C, 50 μL AmDH cell extract. [b]n.d. = not detected.

Herein, a novel AmDH for the asymmetric synthesis of long-chain aliphatic amines was discovered and subsequently optimized through structurally based mutagenesis to enhance its catalytic efficiency and substrate tolerance. For satisfying the requirements of industrial synthesis, the best AmDH mutant was coupled with glucose dehydrogenase (GDH) to achieve the reductive amination process successively without the supplement of NADH. Subsequently, this system was integrated with Au-catalyzed hydration reactions in a one-pot sequential cascade system, enabling the direct conversion of inexpensive alkynes into chiral amines, offering a promising alternative route for the production of chiral aliphatic amines (Figure 2C).

2. RESULTS AND DISCUSSION

2.1. Mining of Amine Dehydrogenases

Given the structural similarity of catalytic substrates, a representative leucine dehydrogenase (LeuDH) from *L. fusiformis*[14] was chosen as the starting template to identify new AmDH candidates for the asymmetric synthesis of long-chain aliphatic amines. Using a BLAST search, the sequences with 40−80% identity (excluding *Escherichia coli*) were collected from the NCBI database. After sequence redundancy and phylogenetic tree analysis, 57 sequences were selected for further sequence alignment (Figure S1).

Based on the above, 8 sequences from distinct branches were selected as candidates. Sequence alignment results revealed that certain amino acid residues, especially those located in the active pocket, were highly conserved, such as the residues corresponding to K68, K80, D115, and N261 in the template *Lf*LeuDH (Figures 3 and S2). Previous reports have indicated that the amino group of leucine interacts with residue D115, while the carboxyl group interacts with residues K68 and K80. This interaction facilitates substrate binding in the active pocket and subsequent reaction processing.[29,30] Upon mutation of K68 to Ser (S) and N261 to Leu (L), the resulting mutant exhibited AmDH activity.[31]

To acquire the ability to catalyze the reductive amination of ketones, two residues in these candidates, corresponding to K68 and N261 of *Lf*LeuDH, were mutated to construct AmDHs (K68S/N261L).[31] The activities of these AmDHs were tested with 4 different long-chain aliphatic ketones, and the AmDH from *Pueribacillus theae* (*Pt*AmDH-M0, K68S/N261L) displayed significant reductive amination activity when the number of side-chain carbons in the substrate was up to seven (Table S3). Also, *Pt*AmDH-M0 showed good stability under alkaline conditions (Figure S4C,D), thus being a potential candidate for further engineering.

2.2. Protein Engineering of *Pt*AmDH

To broaden the substrate scope of *Pt*AmDH-M0, its structure model was built based on the crystal structure of LeuDH from *Lysinibacillus sphaericus* (PDB code: 1LEH) with a sequence similarity of 70% and docked with the active substrates **1a**−**3a** (**1a**: 2-pentanone, **2a**: 2-hexanone, **3a**: 2-heptanone) and the nonactive substrates **4a**−**5a** (**4a**: 2-octanone, **5a**: 2-nonanone), respectively. In *Pt*AmDH-M0, substrates **1a**−**3a** all exhibited similar conformations, in which the carbonyl group of each substrate was close to the K80 and the aliphatic chain was securely accommodated within the cavity formed by L40, A113, E114, D115, T134, V291, and V294. In contrast to substrates **1a**−**3a**, substrates **4a** and **5a** assumed distinct and unstable conformations due to the steric hindrance imposed by their longer carbon chains, consequently leading to their lack of activity. (Figures 4 and S9) Thus, increasing the volume of the binding cavity for the aliphatic chains may be beneficial for improving the enzymatic activity against these long-chain substrates.

We inspected the amino acids encompassing the active pocket of *Pt*AmDH-M0 utilizing HotSpot Wizard,[32] to extract the amino acid hotspots (excluding the catalytic residues K80 and D115) and cross-referenced with the outcomes of molecular docking, thus suggesting that five amino acids neighboring the active pockets may possibly influence their steric hindrance (namely, L40, A113, T134, V291, and V294). Consequently, these five amino acids were mutated to smaller Gly and Ala, respectively. As expected, the obtained mutants A113G, T134G, V291A, V291G, V294A, and V294G all showed improved activity against the long-chain aliphatic ketones. For example, the mutant A113G displayed activity toward the previously nonactive substrates **4a** and **5a**, and the specific activity against **3a** was also increased to 320.4 $U/g_{protein}$ about 10-fold higher than that of *Pt*AmDH-M0. The pocket analysis of A113G revealed that its volume was increased to 733.8 $Å^3$ from 711.9 $Å^3$ of the *Pt*AmDH-M0. Similar phenomena were also observed in the other mutants. However, mutating L40 to small amino acids (A or G) yielded unsatisfactory results. Although the active pocket volume of L40A (730.3 $Å^3$) or L40G (747.9 $Å^3$) was larger than that of M0 (711.9 $Å^3$), the activity decreased or was even completely lost. The mutations of L40 primarily affected the depth of the

https://doi.org/10.1021/jacsau.4c00222
JACS Au 2024, 4, 2281−2290

Table 2. Kinetic Parameters of *Pt*AmDH-M0 and the Triple Mutant toward Different Aliphatic Substrates 1a−5a

entry	mutant	substrate	K_M (mM)	k_{cat} (s^{-1})	k_{cat}/K_M (s^{-1} mM^{-1})
1	*Pt*AmDH-M0	**1a**	9.02 ± 1.38	0.895	0.099
2		**2a**	19.42 ± 2.49	0.428	0.022
3		**3a**	25.71 ± 4.73	0.211	0.008
4		**4a**	n.d.	n.d.[a]	n.d.
5		**5a**	n.d.	n.d.	n.d.
6	*Pt*AmDH (A113G/T134G/V294A)	**1a**	21.89 ± 2.17	0.545	0.025
7		**2a**	15.64 ± 2.37	1.193	0.076
8		**3a**	10.05 ± 1.02	1.011	0.101
9		**4a**	26.53 ± 3.56	0.273	0.011
10		**5a**	31.14 ± 5.39	0.284	0.009

[a]n.d. = not detected.

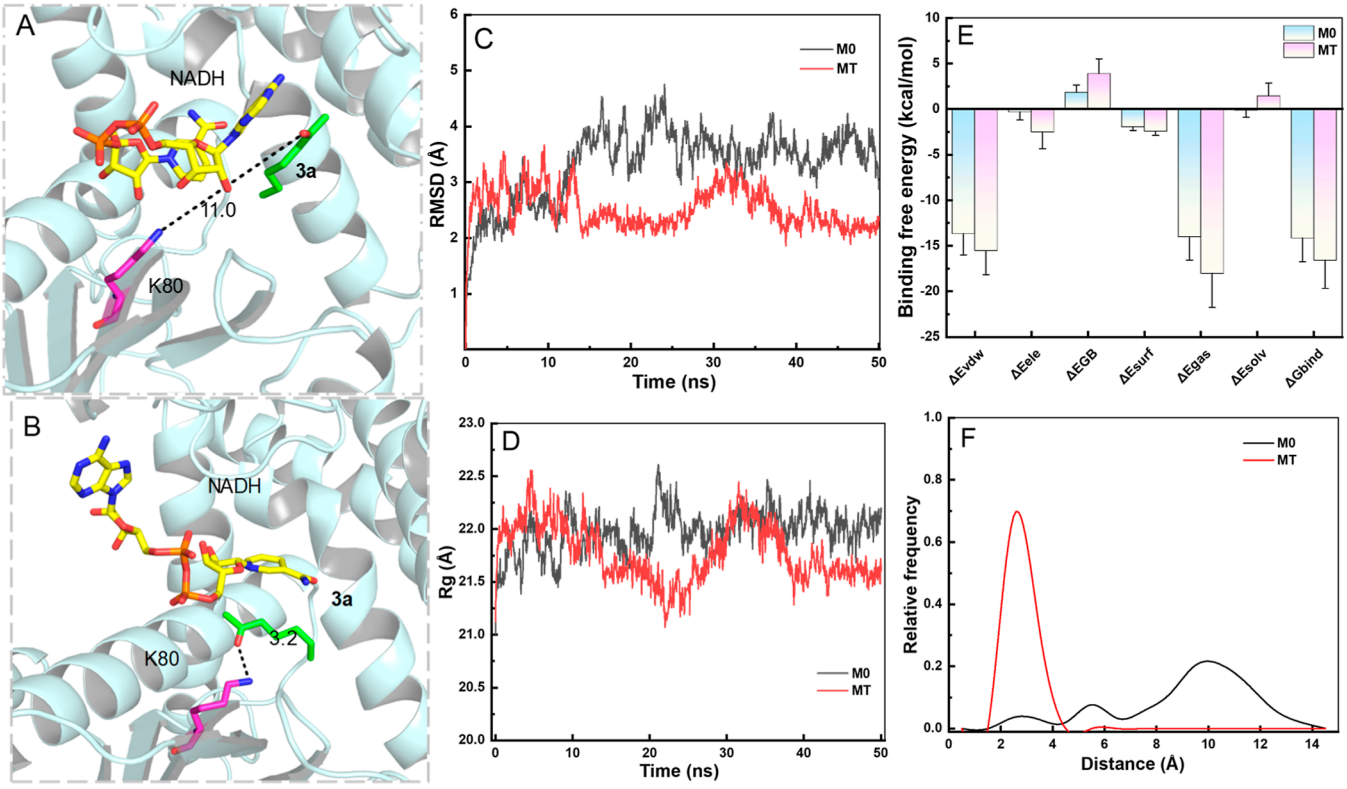

Figure 5. Molecular dynamics simulation. (A) Distance between substrate and K80 in the M0 system at 50 ns; (B) distance between substrate and K80 in the mutant protein system at 50 ns; (C) RMSD range statistics; (D) R_g range statistics; (E) comparison of binding free energy. (F) Comparison of distance distribution relative frequency between substrate and K80. (M0: *Pt*AmDH-M0).

active pocket. Compared with the L40 mutants, other mutants, e.g., A113G, mainly contributed to increasing the width of the active pocket to accommodate long side chains of aliphatic substrates (Tables 1 and S4). Overall, the increasing width of the pocket of *Pt*AmDH-M0 by mutating gatekeeper residues into small amino acids enables the effective alleviation of steric hindrance caused by long side chains and improves activity, but blindly enlarging the depth of the pocket may lead to adverse effects.

To further enhance the activity toward long-chain aliphatic ketones, the beneficial mutations were combined to yield several combinatorial mutants. As shown in Table 1, all the combinatorial mutants displayed good activities toward **4a** and **5a**, and the triple mutant A113G/T134G/V294A exhibited the best activity of 192.1 and 152.8 $U/g_{protein}$, respectively. (Table 1) Thus, residues 113, 134, and 294 exhibited additive effects on the activity of *Pt*AmDH.

2.3. Kinetic Parameters

To evaluate the catalytic ability of the triple mutant A113G/T134G/V294A, its kinetic parameters were determined against different substrates and compared with those of the *Pt*AmDH-M0. (Figure S13 and Table 2) The mutant A113G/T134G/V294A exhibited improved activity against all aliphatic ketones containing more than 5 carbons. Beyond the broader substrate scope, the catalytic efficiency (k_{cat}/K_M) of the mutant A113G/T134G/V294A against **2a** and **3a** increased 3.5-fold and 12.5-fold, respectively, resulting from both the decrease of K_M and the increase of k_{cat}. (Table 2) Therefore, for the long-chain substrates, the mutations toward small amino acids of residues 113, 134, and 294 have direct effects on the activity of *Pt*AmDH by increasing substrate affinity and catalytic efficiency.

https://doi.org/10.1021/jacsau.4c00222
JACS Au 2024, 4, 2281−2290

2.4. Molecular Mechanism of Improved Activity

To explore the mechanism of the improved activity against the long-chain substrates, the active substrates (**2a**−**3a**) and the substrates that *Pt*AmDH-M0 cannot catalyze (**4a**−**5a**) were docked into the triple mutant A113G/T134G/V294A, respectively, and compared with the docking results of *Pt*AmDH-M0. Molecular docking results revealed that the binding modes of substrates **2a**−**3a** were similar in *Pt*AmDH-M0 and the triple mutant A113G/T134G/V294A, while the binding modes of the long-chain substrates (**4a**−**5a**) were obviously different in the two enzymes. For *Pt*AmDH-M0, the long-chain substrates (**4a**−**5a**) adopted inactive conformations with the bulky side chain located outside the pocket of *Pt*AmDH-M0, due to the steric hindrance of residues A113, T134, and V294. (Figure 4E,F) For the triple mutant A113G/T134G/V294A, the long aliphatic chains of substrates (**4a**−**5a**) can be accommodated in the larger cavity formed by residues G113, G134, and A294, enabling these substrates to adopt conformations similar to those of substrates **2a**−**3a** possessing shorter aliphatic chains and to be easily catalyzed. In addition, the distance between the carbonyl group and K80 was also reduced (Figure 4I,J).

Meanwhile, the molecular dynamics simulations (MD simulations) were performed using **3a** as the model substrate, to further analyze the dynamic interactions and changes of molecular structures during the reaction process, as well as the reasons for the higher activity.[33−35] In the AmDH-catalyzed reactions, residues K80 and NH_4^+ attack the electrophilic carbon and initiate the reaction; thus, the distance between the carbonyl group of the substrate and residue K80 is a reliable parameter reflecting the reaction activity.[36] In the simulation process within 50 ns, the distance between the carbonyl oxygen atom of **3a** and the amino nitrogen atom of K80 was frequently around 11.0 Å in *Pt*AmDH-M0 and longer than that of the triple mutant (3.2 Å), indicating that the substrate was more easily reduced in the mutant. Meanwhile, the binding free energies of **3a** in *Pt*AmDH-M0 and the triple mutant were calculated as −14.18 and −16.61 kcal/mol, respectively (Figure 5E), suggesting that the affinity between the substrate and enzyme was enhanced after the introduction of the three mutations. These results were consistent with the increased k_{cat} value and the decreased K_M value of the mutant. Additionally, comparisons of the RMSD, RMSF, and R_g values of these two enzymes showed a similar trend, and the three indexes of the triple mutant were lower than those of the *Pt*AmDH-M0 during the whole simulation (Figures 5 and S23), suggesting that the conformation of the triple mutant after substrate binding was more stable and beneficial to increase the activity (Figures 5 and S23).

Overall, the three mutations not only are favorable for the substrate binding in the positive conformations via eliminating the steric hindrance of residues A113, T134, and V294 but also facilitate the reaction process more easily via shortening the distance between the carbonyl group of the substrate and residue K80, lowering the binding free energy as well as increasing the structural stability.

2.5. Construction of a NADH-Regeneration System for Successive Reductive Amination of High Concentration Ketones

Given the large consumption of NADH in the successive synthesis of chiral amines, an AmDH-GDH cascade was constructed. To improve the catalytic efficiency, the ratio of the two enzymes, the amount of cosubstrate glucose, as well as the type of the cosolvents and their addition amounts were optimized, respectively. Taking 5 g/L (50 mM) **2a** as a model, when GDH/AmDH was 1.25 (U/U) and 20 g/L glucose was added, the yield is the highest (Figures S10 and S11). To increase the solubility of the long-chain substrates, five types of cosolvents were screened[37−39] (Figure S12), and three cosolvents with good effects were selected to further optimize their addition amount (Table S5). It was found that strong hydrophobic cosolvents are better than others, and the mixture of 5% heptane and 5% 2-propanol as the cosolvent showed the most positive effect.

Under optimal conditions, asymmetric reductive amination of **2a** was performed at concentrations ranging from 100 to 2000 mM. (Figure S14) For all the tested concentrations, the synthesis of chiral amines was carried out successively, and the yield reached more than 88% within 16 h when the substrate concentrations were below 800 mM, producing a maximum yield of 71 g/L. Also, the AmDH-GDH coupled system showed good conversion performance against other substrates at the high concentrations, which catalyzed **1**−**5a** at 400 mM with a yield of more than 70% and excellent ee values of 99%.

To verify the universality of the mutant A113G/T134G/V294A, its catalytic activity was also evaluated using more long-chain aliphatic ketones, various cyclic ketones, and aromatic ketones as substrates. (Figure 6) Compared with *Pt*AmDH-M0, the mutant A113G/T134G/V294A displayed better catalytic activity against all the tested substrates. Taking the dietary supplements **6b**, **7b**, and **8b** as examples, the yields of products reached more than 35 g/L when 50 g/L substrates were added, providing a new synthetic route to dietary

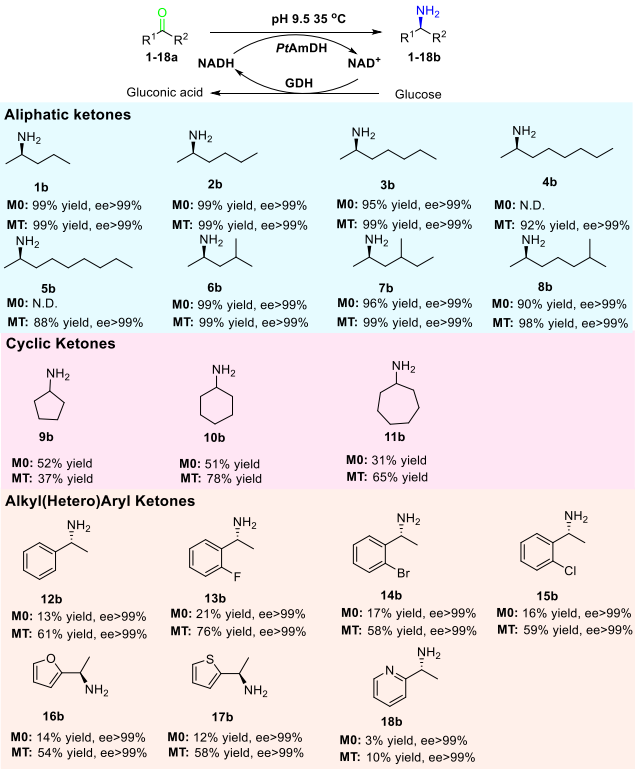

Figure 6. Direct asymmetric reductive amination of different ketones using *Pt*AmDH-M0 (M0) and engineered *Pt*AmDH (A113G/T134G/V294A) (MT). N.D. = not detected.

https://doi.org/10.1021/jacsau.4c00222
JACS Au 2024, 4, 2281−2290

supplements and avoiding precious-metal catalysis. The mutant led to a 2-fold improvement in the yield for **11a** which was up to 65%. Notably, *Pt*AmDH (A113G/T134G/V294A) showed obviously improved activities toward alkyl(hetero)aryl ketones **12a**−**17a**. The yields reached more than 54%, which were 3−5 fold higher than those of *Pt*AmDH-M0. Structural comparison of the *Pt*AmDH mutant and *Pt*AmDH-M0 revealed that, upon the introduction of these three mutations, the size of the active pocket was increased [*Pt*AmDH (A113G/T134G/V294A) 793.5 $Å^3$ vs *Pt*AmDH-M0 711.9 $Å^3$], as well as its hydrophobicity was enhanced, probably beneficial for the binding of aromatic ketones. (Figure S23B) Molecular docking results also showed that the active pocket of the *Pt*AmDH mutant could accommodate the substrate in better binding modes (Figure S15). Thus, the high substrate tolerance and the wide substrate scope of the AmDH-GDH coupled system make it more suitable for industrial application.

2.6. Recyclable Gold-Catalyzed Hydration of Alkynes

As indispensable precursors of chiral aliphatic amines, aliphatic ketones are preferably prepared by more effective and economical synthetic methods. Au-catalyzed alkyne hydration is a considerable approach in the synthesis of ketones due to its high atom economy as well as the easy availability and low cost of alkynes.[40,41] However, there have been a few reports focusing on the hydration of aliphatic alkynes. As such, the development of effective aliphatic alkyne hydration and its further integration with AmDHs in a one-pot cascade reaction enable the direct conversion of cheap alkynes into chiral aliphatic amines, presenting great potential in industrial applications.

Given the inhibitory effect and cost of the Au catalyst, a recyclable catalyst capable of converting the aliphatic alkynes into ketones was designed. Au−HS@SO_3H−PMO(Et) reported by Li[42] displayed good catalytic ability toward all the tested aliphatic alkynes and reusability.

HAADF-STEM results revealed that Au nanoparticles were well dispersed in Au@HS/SO_3H−SiO_2, (Figure S16A−F) in which the loading of Au NPs was up to 2.3 wt % determined using inductively coupled plasma emission spectrometry, and the average particle size was small, mostly around 1.3 nm (Figure S17B). XPS spectra showed that Au in Au@HS/SO_3H−SiO_2 existed at Au(0), corresponding to the binding energy (B.E.) of 84.6 eV in $4f_{7/2}$ Au (Figure S16G). The results of Figure S16H showed that S had two oxidation states of +2 and +6, corresponding to the −SH and $-SO_3H$, respectively, and B.E. was about 163.5 and 167.4 eV in the S 2p, respectively, suggesting that the Au@HS/SO_3H−SiO_2 catalyst was successfully prepared.[42]

Subsequently, the conditions for Au catalysis were optimized by adjusting parameters such as temperature, solvent, and time (Table 3). Given the compatibility with the following enzyme catalysis and the promoting roles in the alkyne hydration reactions, 20% 2-propanol was chosen as a cosolvent to enhance substrate solubility in the system. When the temperature reached more than 70 °C, **3b** could be completely generated within 2.5 h.

2.7. Construction of the Au-AmDH Cascade Catalytic System

As we have previously established a method for converting aliphatic alkyne **3j** to the corresponding ketone **3a**, we attempted to combine Au catalysis with enzymatic catalysis in a one-pot, one-step system. Unfortunately, no satisfactory result was obtained. The results showed that Au was not compatible with the enzyme, and the overall yield was only 27% (Table S6), which is mainly due to two reasons. First, the activity of *Pt*AmDH was seriously impacted by Au@HS/SO_3H−SiO_2, only 25% of the initial enzyme activity can be retained after coincubation with Au-catalyst for 20 h. Second, the catalytic activity of the Au catalyst was reduced in NH_4Cl/$NH_3·H_2O$ buffer with a high salt concentration. (Table 3) To solve the incompatibility issue between metal and enzyme, we tried a one-pot, two-step approach to separate metal and enzyme catalysts by temporal compartmentalization. The reaction mixture of the Au-catalyzed alkyne hydration can be directly used for the further biosynthesis of the target amino product **3b** catalyzed by the *Pt*AmDH mutant only after simple centrifugation. As expected, we got satisfactory results with a yield of 98%, ee >99%. We monitored the progress of the Au-AmDH cascade catalytic system. The experimental results showed that **3j** (100 mM) can be almost completely converted to **3b** within 19 h. (Figure S18) Meanwhile, the recyclable catalyst Au@HS/SO_3H−SiO_2 showed good reusability (Figure S19), which not only can maintain a yield of over 90% even after 6 times of reuse but also remains less than 0.01% in the reaction mixture determined by the ICP test, thus in line with the concept of green sustainability.

Table 3. Catalytic Performance of Au@HS/SO_3H−SiO_2 for the 3j Hydration Reaction[a,b]

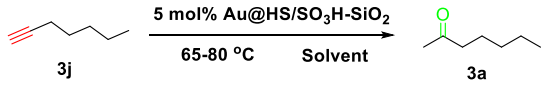

entry	temperature (°C)	solvent (v/v)	time (h)	yield (%)[a]
1	80	20% 2-propanol	3.5	99
2	75	20% 2-propanol	3.5	99
3	70	20% 2-propanol	3.5	99
4	65	20% 2-propanol	3.5	87
5	70	H_2O	3.5	90
6	70	buffer[b]	3.5	51
7	70	10% 2-propanol	3.5	95
8	70	30% 2-propanol	3.5	93
9	70	20% 2-propanol	2.5	99
10	70	20% 2-propanol	2	98
11	70	20% 2-propanol	1.5	93
12	70	20% 2-propanol	1	87

[a]Yield was measured by GC analyses. Reaction conditions: 20 mM **3j**, 5 mol % Au@HS/SO_3H−SiO_2. [b]buffer: pH 9.5 1 M NH_4Cl/$NH_3·H_2O$.

2.8. Gram Synthesis of Chiral Amines in a Au-AmDH One-Pot, Two-Step System

Having constructed the Au-AmDH cascade system for the direct synthesis of chiral amines from alkynes, we extended this system to synthesize more aliphatic amines and various alkyl(hetero)aryl amines on a large scale. To our satisfaction, except for short aliphatic product **1b** affected by its effumability, gram-scale syntheses of all other products **2b**−**8b** were achieved through this cascade system, with yields over 80% and excellent ee values (>99%). The yield of **2b**−**8b** (100 mM) could reach up to 36−60 g/L when 500 mM aliphatic alkynes was added. Moreover, more than 25 g/L of alkyl(hetero)arylamines was also obtained using the corresponding alkynes as raw materials (Figure 7).

https://doi.org/10.1021/jacsau.4c00222
JACS Au 2024, 4, 2281−2290

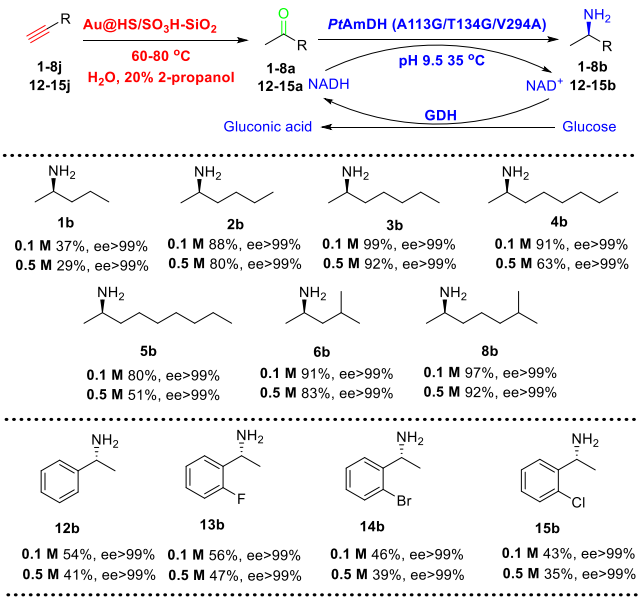

Figure 7. Chemoenzymatic cascade catalyzed hydrating amination of alkynes.

3. CONCLUSIONS

In conclusion, a chemoenzymatic cascade system specific for the synthesis of long-chain aliphatic amines was constructed, which catalyzed the direct conversion of various aliphatic alkynes to the corresponding chiral amines with excellent ee (>99%), and the product yields were all more than 57% at high alkyne concentrations. In particular, the yields of (*R*)-2-heptamine and (*R*)-6-methyl-2-heptamine reached up to 60 g/L. To adapt the reductive amination of aliphatic ketones, a new AmDH was mined and engineered by using structure-guided mutagenesis. The best mutant *Pt*AmDH (A113G/T134G/V294A) can catalyze the asymmetric reductive amination of the long-chain aliphatic ketone substrates at 400 mM with yields of more than 70% (ee >99%). Molecular docking and molecular dynamics simulations confirmed the importance of "gatekeepers" on the catalytic activity, namely residues 113, 134, and 294. This study presents a green and efficient one-pot sequential cascade system for directly converting inexpensive alkynes into chiral long-chain aliphatic amines in aqueous solutions, further demonstrating the potential significance and availability of chemo-enzymatic cascade in large-scale industrial synthesis.

4. EXPERIMENTAL SECTION

4.1. Mining of Amine Dehydrogenases

The *Lf*AmDH from *L. fusiformis* was used as the template to conduct a protein BLAST search in the NCBI database, and sequences with 40−80% homology were selected (*E. coli* and strains reported in the literature were excluded). Through the Novopro website (https://www.novopro.cn/tools/prot-sol.html) for the analysis of soluble protein sequences, select solubility values greater than 0.46 sequence for the construction of the evolutionary tree, through pairwise sequence alignment, remove redundant sequences. The obtained evolutionary tree was further screened, and sequence alignment analysis was performed to select the appropriate proteins for expression verification.

4.2. Prediction of Amino Acid Hotspots

The three-dimensional (3D) structure of *Pt*AmDH-M0 was constructed from the SWISS-MODEL web server (https://swissmodel.expasy.org) by using LeuDH from *L. sphaericus* (PDB code: 1LEH) as the template. Different substrates (**1a**−**5a**) were docked into the active pocket of *Pt*AmDH-M0. K80 and D115 of *Pt*AmDH-M0 were set as the center of the grid box, and the size of the gridbox in each direction was set as 40. 100 docking poses were set for each substrate. The sequence of *Pt*AmDH-M0 was also submitted to HotSpot Wizard 3.0, and the hot spots were predicted by using the function of consensus sequence computation in HotSpot Wizard 3.0 (https://loschmidt.chemi.muni.cz/hotspotwizard/).

4.3. Construction, Expression, and Purification of *Pt*AmDH and Its Mutants

The gene *Pt*AmDH was cloned into plasmid pET28a(+) and then transformed into *E. coli* BL21(DE3) cells for protein expression. To obtain the expression plasmids of the *Pt*AmDH mutants, PCR was performed using primers (Table S2) and plasmid pET28a(+)-*Pt*AmDH as the template DNA with KOD plus DNA polymerase. The PCR products were digested by *Dpn* I and transformed into *E. coli* DH5α for amplification. All plasmids harboring mutated genes were verified by sequencing and transformed into *E. coli* BL21(DE3) cells.

The protein expression of *Pt*AmDH and its mutants was induced by isopropyl-β-thiogalactopyranoside (IPTG). *Pt*AmDH was purified on a HisTrap chelating HP column (GE Healthcare). Detailed experimental methods are provided in the Supporting Information.

4.4. Enzyme Activity Assay

The activity of *Pt*AmDH and its mutants was measured by monitoring the change in the absorbance at 340 nm using a SpectraMax 190 (Molecular Devices, USA). The activity assay was carried out in 1 mL of reaction mixture containing $NH_4Cl/NH_3{\cdot}H_2O$ buffer (2 M, pH 9.5), 0.2 mM NADH, 20 mM substrate, and an appropriate concentration of enzyme at 30 °C. One unit activity (1 U) was defined as the amount of enzyme that catalyzed the conversion of 1 μmol NADH during 1 min.

4.5. Kinetic Assay

Kinetic parameters toward ketone substrates were determined with varied ketone substrate concentrations by using the activity assay method described above. The substrate concentration was varied from 0 to 80 mM while keeping the NADH and ammonia concentrations fixed. Kinetic parameters (K_M and k_{cat}) were calculated by nonlinear curve fitting of initial velocity versus substrate concentration data to the Michaelis−Menten equation.

4.6. Molecular Dynamics Simulation

Gromacs 5.1.5 was used in this study for molecular dynamics. The simulation system was set in a closed environment with 289.15 K, pH 9.5, and 1 bar. The periodic boundary setting of the simulation system was centered on the protein, and the minimum distance between the protein edge and the box edge was set as 0.1 nm. The GAFF force field was used to deal with ligand atoms. TIP3P water molecules were added to simulate the water environment, and NaCl was used to balance the system charge. After building the initial system, it will use the steepest descent method for all atoms to minimize the system's energy. Constant number of particles, volume, and temperature (*NVT*), and constant number of particles, pressure, and

https://doi.org/10.1021/jacsau.4c00222
JACS Au 2024, 4, 2281−2290

temperature (*NPT*) (1000 ps). After *NVP* and *NPT* balance, the *Pt*AmDH-M0 and mutant systems were simulated for 50 ns of finished product dynamics, and the system was simulated every 2 fs.

4.7. Preparation of Chiral Amines Using *Pt*AmDH (A113G/T134G/V294A)

50 mM **1−18a** was added into the reaction system (10 mL) and reacted for 16−20 h. The product was extracted by ethyl acetate/methyl *tert*-butyl ether and the yield was determined by GC. Reaction system: 1.25 mL *Pt*AmDH (A113G/T134G/V294A), 1 mL GDH, 0.25 mM NAD^+, pH 9.5, 35 °C. NMR: the solvent was evaporated under reduced pressure, and the remaining residue was dissolved in distilled water (20 mL). The solution was acidified to pH 1 with concentrated HCl and then washed with EtOAc (3 × 20 mL), discarding the organic layer. Then, the aqueous phase was basified to pH = 12 with an aqueous NaOH 10 M solution (5 mL) and extracted with CH_2Cl_2 (3 × 20 mL). The organic layers were combined, dried over Na_2SO_4, and filtered, and the solvent was evaporated under reduced pressure.

4.8. Optimization of Conditions for Alkynes' Hydration Catalyzed by Au@HS/SO_3H−SiO_2

3j was taken as the model substrate, with the following reaction conditions: 20 mM **3j**, 5 mol % Au@HS/SO_3H−SiO_2. Temperature, solvent, and reaction time were adjusted. The products were extracted by ethyl acetate. The yield was determined by GC.

4.9. Preparation of Chiral Amines from Alkynes Using Chemoenzymatic Cascade Reactions

In the first step (hydration reaction), 100 mM alkyne (**1−8j**, **12−15j**) was added to a 5 mL system; then, 20% 2-propanol and 5 mol % Au@HS/SO_3H−SiO_2 were added and reacted for 2.5 h. In the second step (asymmetric reduction amination), the insoluble matter was removed by centrifugation, and 5 mL of $NH_4Cl/NH_3{\cdot}H_2O$ buffer (4 M, pH 9.5), 1.25 mL *Pt*AmDH (A113G/T134G/V294A), 1 mL GDH, 4 equiv glucose, and 0.25 mM NAD^+ were added and reacted at 35 °C for 16 h. The products were extracted by ethyl acetate/methyl *tert*-butyl ether. The yield was determined by GC.

Also, the scale-up preparation was carried out at the concentrations of 500 mM alkynes (**1−8j** and **12−15j**) with other reaction conditions remaining unchanged.

■ ASSOCIATED CONTENT

Supporting Information

The Supporting Information is available free of charge at https://pubs.acs.org/doi/10.1021/jacsau.4c00222.

General information, preparation of amine dehydrogenases, procedures for molecular docking simulations, supplementary figures, synthesis of substrates, GC, and ^1H and ^{13}C NMR spectra (PDF)

■ AUTHOR INFORMATION

Corresponding Authors

Jing Bai − *College of Food Science and Biology, Hebei University of Science & Technology, Shijiazhuang 050018, China*; Email: Baijing@hebust.edu.cn

Yanjun Jiang − *School of Chemical Engineering and Technology, Hebei University of Technology, Tianjin 300130, China*; orcid.org/0000-0003-1470-2102; Email: yanjunjiang@hebut.edu.cn

Authors

Jianqiao Liu − *School of Chemical Engineering and Technology, Hebei University of Technology, Tianjin 300130, China*

Yunting Liu − *School of Chemical Engineering and Technology, Hebei University of Technology, Tianjin 300130, China*; orcid.org/0000-0003-3799-0362

Liya Zhou − *School of Chemical Engineering and Technology, Hebei University of Technology, Tianjin 300130, China*

Ying He − *School of Chemical Engineering and Technology, Hebei University of Technology, Tianjin 300130, China*; orcid.org/0000-0002-8857-3545

Li Ma − *School of Chemical Engineering and Technology, Hebei University of Technology, Tianjin 300130, China*

Guanhua Liu − *School of Chemical Engineering and Technology, Hebei University of Technology, Tianjin 300130, China*; orcid.org/0000-0002-0824-9738

Jing Gao − *School of Chemical Engineering and Technology, Hebei University of Technology, Tianjin 300130, China*

Complete contact information is available at: https://pubs.acs.org/10.1021/jacsau.4c00222

Notes

The authors declare no competing financial interest.

■ ACKNOWLEDGMENTS

This work was supported by the National Key Research and Development Program of China (2023YFA0914500), the National Natural Science Foundation of China (No 22178083 and 22078081), the Natural Science Foundation of Hebei Province (B2022202014), S&T Program of Hebei (21372804D), and the Science and Technology Research Project of Hebei Higher Education (JZX2023012). The authors would also like to thank Shiyanjia Lab (www.shiyanjia.com) for the MD.

■ REFERENCES

(1) Cai, R. F.; Liu, L.; Chen, F. F.; Li, A. T.; Xu, J. H.; Zheng, G. W. Reductive amination of biobased levulinic acid to unnatural chiral γ-Amino acid using an engineered amine dehydrogenase. *ACS Sustain. Chem. Eng.* **2020**, *8* (46), 17054−17061.

(2) Senthamarai, T.; Murugesan, K.; Schneidewind, J.; Kalevaru, N. V.; Baumann, W.; Neumann, H.; Kamer, P. C. J.; Beller, M.; Jagadeesh, R. V. Simple ruthenium-catalyzed reductive amination enables the synthesis of a broad range of primary amines. *Nat. Commun.* **2018**, *9* (1), 4123.

(3) Murugesan, K.; Senthamarai, T.; Chandrashekhar, V. G.; Natte, K.; Kamer, P. C. J.; Beller, M.; Jagadeesh, R. V. Catalytic reductive aminations using molecular hydrogen for synthesis of different kinds of amines. *Chem. Soc. Rev.* **2020**, *49* (17), 6273−6328.

(4) Chen, F.-F.; Cosgrove, S. C.; Birmingham, W. R.; Mangas-Sanchez, J.; Citoler, J.; Thompson, M. P.; Zheng, G.-W.; Xu, J.-H.; Turner, N. J. Enantioselective synthesis of chiral vicinal amino alcohols using amine dehydrogenases. *ACS Catal.* **2019**, *9* (12), 11813−11818.

(5) Liu, T. L.; Wang, C. J.; Zhang, X. Synthesis of chiral aliphatic amines through asymmetric hydrogenation. *Angew. Chem., Int. Ed. Engl.* **2013**, *52* (32), 8416−8419.

(6) Guo, F.; Berglund, P. Transaminase biocatalysis: optimization and application. *Green Chem.* **2017**, *19* (2), 333−360.

(7) Wang, D. H.; Chen, Q.; Yin, S. N.; Ding, X. W.; Zheng, Y. C.; Zhang, Z.; Zhang, Y. H.; Chen, F. F.; Xu, J. H.; Zheng, G. W. Asymmetric reductive amination of structurally diverse ketones with ammonia using a spectrum-extended amine dehydrogenase. *ACS Catal.* **2021**, *11* (22), 14274−14283.
(8) Wang, J. W.; Li, Y.; Nie, W.; Chang, Z.; Yu, Z. A.; Zhao, Y. F.; Lu, X.; Fu, Y. Catalytic asymmetric reductive hydroalkylation of enamides and enecarbamates to chiral aliphatic amines. *Nat. Commun.* **2021**, *12* (1), 1313.
(9) Citoler, J.; Derrington, S. R.; Galman, J. L.; Bevinakatti, H.; Turner, N. J. A biocatalytic cascade for the conversion of fatty acids to fatty amines. *Green Chem.* **2019**, *21* (18), 4932−4935.
(10) Feng, M.; Tinelli, R.; Meyrelles, R.; Gonzalez, L.; Maryasin, B.; Maulide, N. Direct Synthesis of α-Amino Acid Derivatives by Hydrative Amination of Alkynes. *Angew. Chem., Int. Ed. Engl.* **2023**, *62* (1), No. e202212399.
(11) Baumler, C.; Bauer, C.; Kempe, R. The synthesis of primary amines through reductive amination employing an iron Catalyst. *ChemSusChem* **2020**, *13* (12), 3110−3114.
(12) Trowbridge, A.; Walton, S. M.; Gaunt, M. J. New strategies for the transition-metal catalyzed synthesis of aliphatic amines. *Chem. Rev.* **2020**, *120* (5), 2613−2692.
(13) Liu, J. Q.; Kong, W. X.; Bai, J.; Li, Y. X.; Dong, L. L.; Zhou, L. Y.; Liu, Y. T.; Gao, J.; Bradshaw Allen, R. T.; Turner, N. J.; et al. Amine dehydrogenases: current status and potential value for chiral amine synthesis. *Chem Catal.* **2022**, *2* (6), 1288−1314.
(14) Chen, F. F.; Zheng, G. W.; Liu, L.; Li, H.; Chen, Q.; Li, F. L.; Li, C. X.; Xu, J. H. Reshaping the active pocket of amine dehydrogenases for asymmetric synthesis of bulky aliphatic amines. *ACS Catal.* **2018**, *8* (3), 2622−2628.
(15) Franklin, R. D.; Mount, C. J.; Bommarius, B. R.; Bommarius, A. S. Separate sets of mutations enhance activity and substrate scope of amine dehydrogenase. *ChemCatChem* **2020**, *12* (9), 2436−2439.
(16) Kang, S. M.; Han, S. S.; Zhu, Y. Y.; Wu, Z. Q. Cobalt(III) porphyrin-decorated stereoregular polyisocyanides enable highly effective cooperative catalysis for hydration of alkynes. *ACS Catal.* **2021**, *11* (22), 13838−13847.
(17) Yuan, T.; Tang, Q.; Shan, C.; Ye, X.; Wang, J.; Zhao, P.; Wojtas, L.; Hadler, N.; Chen, H.; Shi, X. Alkyne trifunctionalization via divergent gold catalysis: combining π-acid activation, vinyl−gold addition, and redox catalysis. *J. Am. Chem. Soc.* **2021**, *143* (10), 4074−4082.
(18) Wang, S.; Miao, C.; Wang, W.; Lei, Z.; Sun, W. Hydration of terminal alkynes catalyzed by a water-soluble salen-Co(III) complex. *Chin. J. Catal.* **2014**, *35* (10), 1695−1700.
(19) Zhou, Z. H.; Zhang, X.; Huang, Y. F.; Chen, K. H.; He, L. N. Synthesis of α-hydroxy ketones by copper(I)-catalyzed hydration of propargylic alcohols: CO_2 as a cocatalyst under atmospheric pressure. *Chin. J. Catal.* **2019**, *40* (9), 1345−1351.
(20) Chen, D. Q.; Guo, C. H.; Zhang, H. R.; Jin, D. P.; Li, X. S.; Gao, P.; Wu, X. X.; Liu, X. Y.; Liang, Y. M. A metal-free transformation of alkynes to carbonyls directed by remote OH group. *Green Chem.* **2016**, *18* (15), 4176−4180.
(21) Xu, Y.; Hu, X.; Shao, J.; Yang, G.; Wu, Y.; Zhang, Z. Hydration of alkynes at room temperature catalyzed by gold(i) isocyanide compounds. *Green Chem.* **2015**, *17* (1), 532−537.
(22) Teles, J. H.; Brode, S.; Chabanas, M. Cationic Gold(I) complexes: highly efficient catalysts for the addition of alcohols to alkynes. *Angew. Chem., Int. Ed.* **1998**, *37* (10), 1415−1418.
(23) de Frémont, P.; Singh, R.; Stevens, E. D.; Petersen, J. L.; Nolan, S. P. Synthesis, characterization and reactivity of N-heterocyclic carbene gold(III) complexes. *Organometallics* **2007**, *26* (6), 1376−1385.
(24) Gatto, M.; Belanzoni, P.; Belpassi, L.; Biasiolo, L.; Del Zotto, A.; Tarantelli, F.; Zuccaccia, D. Solvent-silver-and acid-free NHC-Au-X catalyzed hydration of alkynes. the pivotal role of the counterion. *ACS Catal.* **2016**, *6* (11), 7363−7376.
(25) Dutta, M. M.; Phukan, P. Hydration of alkynes to ketones using cobalt ferrite magnetic nanocatalyst encrusted with gold nanoparticles. *Inorg. Chem. Commun.* **2021**, *133*, 108964.
(26) Chang, F.; Wang, C.; Chen, Q.; Zhang, Y.; Liu, G. A chemoenzymatic cascade combining a hydration catalyst with an amine dehydrogenase: synthesis of chiral amines. *Angew. Chem., Int. Ed. Engl.* **2022**, *61* (10), No. e202114809.
(27) Mathew, S.; Sagadevan, A.; Renn, D.; Rueping, M. One-pot chemoenzymatic conversion of alkynes to chiral amines. *ACS Catal.* **2021**, *11* (20), 12565−12569.
(28) González-Granda, S.; Tzouras, N. V.; Nolan, S. P.; Lavandera, I.; Gotor-Fernández, V. Merging gold(I) catalysis with amine transaminases in cascade catalysis: chemoenzymatic transformation of propargylic alcohols into enantioenriched allylic amines. *Adv. Synth. Catal.* **2022**, *364* (22), 3856−3866.
(29) Sharma, M.; Mangas-Sanchez, J.; Turner, N. J.; Grogan, G. NAD(P)H-dependent dehydrogenases for the asymmetric reductive amination of ketones: structure, mechanism, evolution and application. *Adv. Synth. Catal.* **2017**, *359* (12), 2011−2025.
(30) Sekimoto, T.; Matsuyama, T.; Fukui, T.; Tanizawa, K. Evidence for lysine 80 as general base catalyst of leucine dehydrogenase. *J. Biol. Chem.* **1993**, *268* (36), 27039−27045.
(31) Abrahamson, M. J.; Vazquez-Figueroa, E.; Woodall, N. B.; Moore, J. C.; Bommarius, A. S. Development of an amine dehydrogenase for synthesis of chiral amines. *Angew. Chem., Int. Ed. Engl.* **2012**, *51* (16), 3969−3972.
(32) Li, S. F.; Xie, J. Y.; Qiu, S.; Xu, S. Y.; Cheng, F.; Wang, Y. J.; Zheng, Y. G. Semirational engineering of an aldo-keto reductase *Km*AKR for overcoming trade-offs between catalytic activity and thermostability. *Biotechnol. Bioeng.* **2021**, *118* (11), 4441−4452.
(33) Wang, F.; Zhu, M.; Song, Z.; Li, C.; Wang, Y.; Zhu, Z.; Sun, D.; Lu, F.; Qin, H.-M. Reshaping the binding pocket of lysine hydroxylase for enhanced activity. *ACS Catal.* **2020**, *10* (23), 13946−13956.
(34) Wu, Z.-M.; Xie, F.; Zheng, W.; Liu, C. F.; Lin, C. P.; Zheng, R. C.; Zheng, Y. G. structure-oriented engineering of amidase: modification of twisted access tunnel for efficient synthesis of 2-chloronicotinic acid. *ACS Catal.* **2023**, *13*, 9078−9089.
(35) Wu, T.; Wang, Y.; Zhang, N.; Yin, D.; Xu, Y.; Nie, Y.; Mu, X. Reshaping substrate-binding pocket of leucine dehydrogenase for bidirectionally accessing structurally diverse substrates. *ACS Catal.* **2023**, *13* (1), 158−168.
(36) Tseliou, V.; Masman, M. F.; Bohmer, W.; Knaus, T.; Mutti, F. G. Mechanistic insight into the catalytic promiscuity of amine dehydrogenases: asymmetric synthesis of secondary and primary amines. *ChemBioChem* **2019**, *20* (6), 800−812.
(37) Luan, P.; Liu, Y.; Li, Y.; Chen, R.; Huang, C.; Gao, J.; Hollmann, F.; Jiang, Y. Aqueous chemoenzymatic one-pot enantioselective synthesis of tertiary α-aryl cycloketones *via* Pd-catalyzed C−C formation and enzymatic C=C asymmetric hydrogenation. *Green Chem.* **2021**, *23* (5), 1960−1964.
(38) Hao, Y. C.; Zong, M. H.; Chen, Q.; Li, N. Engineering carbonyl reductase for one-pot chemobiocatalytic enantioselective synthesis of a value-added N-containing chiral alcohol from *N*-acetyl-d-glucosamine. *Green Chem.* **2023**, *25*, 5051−5058.
(39) Au, S. K.; Bommarius, B. R.; Bommarius, A. S. Biphasic Reaction System Allows for Conversion of Hydrophobic Substrates by Amine Dehydrogenases. *ACS Catal.* **2014**, *4* (11), 4021−4026.
(40) Zuccaccia, D.; Del Zotto, A.; Baratta, W. The pivotal role of the counterion in gold catalyzed hydration and alkoxylation of alkynes. *Coord. Chem. Rev.* **2019**, *396*, 103−116.
(41) Venkateswara Rao, K. T.; Sai Prasad, P. S.; Lingaiah, N. Solvent-free hydration of alkynes over a heterogeneous silver exchanged silicotungstic acid catalyst. *Green Chem.* **2012**, *14* (5), 1507.
(42) Zhu, F. X.; Wang, W.; Li, H. X. Water-medium and solvent-free organic reactions over a bifunctional catalyst with Au nanoparticles covalently bonded to HS/SO_3H functionalized periodic mesoporous organosilica. *J. Am. Chem. Soc.* **2011**, *133* (30), 11632−11640.

https://doi.org/10.1021/jacsau.4c00222
JACS Au 2024, 4, 2281−2290